From diffusion signal moments to neurite diffusivities, volume fraction and orientation distribution: An exact solution

Dmitry S. Novikov[1], Ileana O. Jelescu[1], and Els Fieremans[1]
[1]*Center for Biomedical Imaging, Department of Radiology, NYU School of Medicine, New York, NY, United States*

Purpose: **To determine brain microstructure parameters from dMRI signal moments, thereby avoiding nonlinear fitting.** Quantifying brain microstructure from dMRI is challenging. While dMRI signal is a fairly featureless function in the *q*-space, the number of parameters necessary to characterize multi-compartmental diffusion in the brain[1-4] can easily exceed 10, making this problem prone to *overfitting*. Nonlinear fitting in such parameter space generally fails, especially at clinically-limited SNR, even with a number of *q*-space points exceeding the number of parameters by an order of magnitude. This is a **fundamental problem**, which severely limits our ability to quantify tissue properties in the clinic, and so far has only been avoided by fixing most of model parameters to *a priori* values[3,5]. An alternative to nonlinear fitting is to relate the low-*b* metrics, such as diffusion and kurtosis tensors, to parameters of nonlinear models; however, this has only been done in a simple geometry of a well-aligned fiber bundle[6] that does not represent most of the brain. **Here we relate *all* diffusion signal moments to *all* fiber orientation and structure characteristics exactly, reducing parameter estimation to a linear problem.**

Methods: We assume a broadly accepted model[1-4] of dMRI signal S in direction $\mathbf{g}$, representing neurites (axons and dendrites) by straight segments, which are characterized by diffusivities D_a (inside), $D_e^{\parallel}$ and $D_e^{\perp}$ (outside), neurite water fraction f, and orientation distribution function (ODF) $\mathcal{P}(\mathbf{n})$:

$$S_{b,\mathbf{g}} = \int \mathrm{d}\mathbf{n}\,\mathcal{P}(\mathbf{n})\left[f e^{-bD_a(\mathbf{n}\cdot\mathbf{g})^2} + (1-f)e^{-bD_e^{\perp}-b\Delta D_e(\mathbf{n}\cdot\mathbf{g})^2}\right] = 1 - bM_{ij}^{(2)}g_ig_j + \frac{b^2}{2!}M_{ijkl}^{(4)}g_ig_jg_kg_l - \frac{b^3}{3!}M_{ijkl}^{(6)}g_ig_jg_kg_lg_mg_n\ldots \qquad \mathcal{P}(\mathbf{n}) = 1 + \sum_{l=2,4,\ldots}\sum_{m=-l}^{l} P_{lm}Y_{lm}(\mathbf{n})$$

Here $\Delta D_e = D_e^{\parallel} - D_e^{\perp}$. We relate these 3+($L_{\max}$+1)($L_{\max}$+2)/2 tissue parameters per voxel, where $L_{\max}$ is the maximum order of spherical harmonics (SH) for the ODF, to the $L_{\max}(L_{\max}+2)(L_{\max}+4)/12+L_{\max}(L_{\max}+6)/8$ components of the fully symmetric moment tensors $M^{(l)}_{k_1\ldots k_l}$ of the signal determined up to l=$L_{\max}$. Here $M^{(2)}$ is the overall diffusion tensor, $M^{(4)}$ is the combination of kurtosis and diffusion tensors, etc. **Our key idea is to work in the basis of symmetric trace-free (STF) tensors**[7] $\mathcal{Y}^{lm}_{k_1\ldots k_l}$ which realize irreducible representations of the rotation group SO(3), and generate SHs $Y_{lm}(\mathbf{n}) = \sqrt{\frac{2l+1}{4\pi}}\mathcal{Y}^{lm}_{k_1\ldots k_l}n_{k_1}\ldots n_{k_l}$. Projecting moments $M^{(L),lm} = \mathcal{Y}^{lm}_{k_1\ldots k_l}\delta_{k_{l+1}k_{l+2}}\ldots\delta_{k_{L-1}k_L}M^{(L)}_{k_1\ldots k_L}$ onto the STF basis, we get the system **(1)** of 5 equations involving the maximally symmetric parts of the 2nd, 4th, and 6th order moments, with 5 unknowns. Here, p_{20} = $(3\langle\cos^2\theta\rangle - 1)/2 \sim Y_{20}(\theta,\varphi)$ is the ODF average of the 2nd Legendre polynomial. **Eqs (1) form the minimal system to determine all compartment diffusivities and neurite water fraction *f*.** The system yields *two branches* of solutions $f_{\pm}(p_{20})$, **Fig. 1**. These branches, at the level of $M^{(2)}$ and $M^{(4)}$, provide a highly degenerate family of solutions, thereby determining **two narrow and sharply-turning trenches in the original multi-dimensional nonlinear optimization landscape (Fig. 1A)**, revealing the fundamental reason of overfitting in brain microstructure models. At this level, the $L_{\max}$=4 case is *indeterminate*, even though 21 diffusion kurtosis imaging (DKI) parameters exceed 18 tissue parameters. Remarkably, the shallow minimum in one of the trenches, **Fig. 1B**, and thereby the solution to the full problem, is only determined after including the 6*th order moment* $M^{(6)}$. This is why only the special case of an aligned fiber bundle can be resolved with DKI alone,[6] and why nonlinear fitting is so sensitive to noise. Once f, D_a, $D_e^{\parallel}$, $D_e^{\perp}$, and p_{20} are found, all other ODF SH coefficients P_{lm} follow from Eq **(2)**, providing the analytical solution up to all orders.

$$\begin{cases} M^{(2),00} = fD_a + (1-f)(3D_e^{\perp} + \Delta D_e) \\ M^{(2),20} = p_{20}\left[fD_a + (1-f)\Delta D_e\right] \\ M^{(4),00} = fD_a{}^2 + (1-f)\left[5D_e^{\perp 2} + \frac{10}{3}D_e^{\perp}\Delta D_e + \Delta D_e{}^2\right] \\ M^{(4),20} = p_{20}\left[fD_a{}^2 + (1-f)\left(\frac{7}{3}D_e^{\perp}\Delta D_e + \Delta D_e{}^2\right)\right] \\ M^{(6),00} = fD_a{}^3 + (1-f)\left[7D_e^{\perp 3} + 7D_e^{\perp 2}\Delta D_e + \frac{21}{5}D_e^{\perp}\Delta D_e{}^2 + \Delta D_e{}^3\right] \end{cases} \quad (1)$$

$$\sqrt{\frac{2l+1}{4\pi}}M^{(l),lm} = P_{lm}\cdot\left[fD_a{}^{l/2} + (1-f)\Delta D_e{}^{l/2}\right] \quad (2)$$

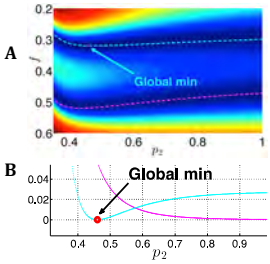

Fig. 1: A, minimization landscape for finding the solution of Eqs (1). **B**, profile along trenches $f_{\pm}(p_{20})$, the roots of a quadratic equation determined after exclusion of 3 diffusivities. Here, f_- gives the true minimum. Eqs (1) are thus reduced to finding a zero, or minimizing, a 1-variable function defined by $M^{(6)00}$

Results: We tested our solution on the ground truth of 3 neurite segments at θ=37° relative to z-axis, with relative weights 2:1:1 and common parameters f=0.32, D_a=1.15, $D_e^{\parallel}$=2.85, $D_e^{\perp}$=1.1 (all units μm and ms), using simulated acquisition of 3 shells x 64 dirs, together with 10 b=0, at both SNR = ∞ and 50. Moments were determined via cumulants using b-matrix pseudoinversion up to $L_{\max}$=6. **Fig. 2** shows that, remarkably, going to too high b-values *reduces accuracy* of the ODF reconstruction, as the moments are less accurately found, while precision suffers at low b due to noise. In **Fig. 3**, we applied our framework to the Human connectome project (HCP) data set. We see that, due to the noise, the choice between the branches $f_{\pm}(p_{20})$ is challenging; sometimes, neither branch has a global minimum. Interestingly, more often the branch with a global minimum is the one where $D_a > D_e^{\parallel}$, especially away from highly aligned tracts. For now, we do not have an insight into the ground truth and the way to select the right branch.

Discussion: We have reduced finding dozens of tissue parameters with nonlinear fitting down to the selection of one of the two branches of an exact relation between diffusion moments and tissue properties. While this selection is still nontrivial, it seems far more promising than relying on nonlinear fitting to find a global minimum in a tortuous high-dimensional space. The fundamental issue of the near-degeneracy of solutions also prompts us to re-optimize dMRI acquisition. On the one hand, 2 shells in the *q*-space (DKI) is not enough. On the other hand, as moments are derivatives of $S(b)$ at b=0, our solution suggests *not* going too far in b, preserving SNR and enabling robust fits of $M^{(l)}_{k_1\ldots k_l}$. Further work will focus on finding an *optimal intermediate multi-shell acquisition range* where the signal is not destroyed, yet enough moments, e.g. $L_{\max}$ ~ 6-8, are determined. With an optimized acquisition, our results can foster clinical translation of advanced dMRI models, as well as serve a starting point for global mesoscopic fiber tracking.[8]

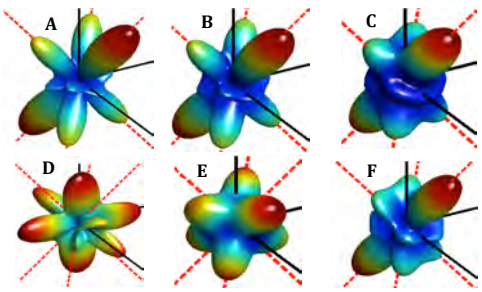

Fig. 2: Effect of SNR and acquisition on ODF. **A-C:** SNR=∞; **D-F:** SNR=50. Shell b-values: **A,D:** 0.1,0.2,0.3; **B,E:** 0.33,0.67,1.0; **C,F:** 1,2,3. Small b give the highest accuracy but the lowest precision in ODF reconstruction.

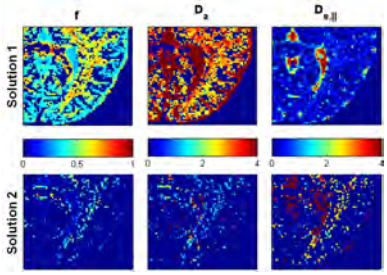

Fig. 3: Application to HCP data (lower quarter of an axial slice). Solutions 1,2 correspond to branches $f_{\pm}$, Fig. 1. Background corresponds to voxels where the branch has no minimum.

References: **1.** Behrens *et al.*, MRM 50, 1077 (2003). **2.** Kroenke *et al.*, MRM 52, 1052 (2004). **3.** Assaf *et al.*, MRM 52, 965 (2004). **4.** Jespersen *et al.*, NeuroImage 34, 1473 (2007); NeuroImage 49, 205 (2010). **5.** Zhang *et al.*, NeuroImage 61, 1000 (2012). **6.** Fieremans *et al.*, NBM 23, 711 (2010); NeuroImage 58, 177 (2011). **8.** Thorne, RevModPhys 52, 299 (1980). **8.** Reisert *et al.*, MICCAI 2014 III-201. Work supported by NIH R01 NS088040.